

Dimer diffusion in a washboard potential

E. Heinsalu,¹ M. Patriarca,¹ and F. Marchesoni²

¹*Institute of Theoretical Physics, University of Tartu, T  he 4, 51010 Tartu, Estonia*

²*Dipartimento di Fisica, Universit   di Camerino, I-62032 Camerino, Italy*

The transport of a dimer, consisting of two Brownian particles bounded by a harmonic potential, moving on a periodic substrate is investigated both numerically and analytically. The mobility and diffusion of the dimer center of mass present distinct properties when compared with those of a monomer under the same transport conditions. Both the average current and the diffusion coefficient are found to be complicated non-monotonic functions of the driving force. The influence of dimer equilibrium length, coupling strength and damping constant on the dimer transport properties are also examined in detail.

PACS numbers: 05.60.-k, 05.40.-a, 68.43.Mn

I. INTRODUCTION

One particular example of Brownian motion on a periodic substrate is the diffusion of atoms and molecules on crystal surfaces [1]. This mechanism is of both conceptual and technological interest [2], being relevant to heterogeneous nucleation, catalysis, surface coating, thin-film growth, etc. Individual atoms diffusing on a surface can eventually meet and form dimers or trimers. For example, on the semiconductor Si(100) or Ge(100) surface, most of the deposited Si or Ge atoms form dimers. Atoms adsorbed on metal surfaces may also form closely packed islands that diffuse as a whole [3, 4, 5]. This raises the issue of the role of the internal degrees of freedom on the transport of extended objects through micro- and submicro-devices.

One of the most important problems in modern nanotechnology is how to manipulate small particles in order to perform a preassigned operation. For instance, the mobility and diffusivity of atoms adsorbed onto crystal surfaces can be controlled by applying deterministic forces [6, 7]. A direct manipulation method consists in applying a constant direct current (dc) local electric field by means of a scanning tunnel microscope tip [8]. A selected adatom or admolecule with nonzero charge will then move in the direction of the electric force; neutral particles will be forced into a region of a stronger field due to induced polarization [9]. This problem can be modeled as a Brownian motion on a tilted periodic two-dimensional (2D) substrate.

In this work we study the transport of a dimer confined on a periodic substrate with a focus on the effects of the internal degrees of freedom on its mobility and diffusivity. For simplicity, we restrict our analysis to substrates in two or higher dimensions, which can be effectively reduced to one-dimensional (1D) systems. In the simple case of a dimer driven by a constant force oriented along a symmetry axis of a 2D substrate, one wants to characterize the stationary transport in the force direction, whereas transverse diffusion is not affected by the bias; for a full 2D treatment, see, e.g., Ref. [10]. Of course, the results of the present paper apply well also

to a variety of physical and biological systems, where the particle dynamics is naturally constrained to (quasi-)1D substrates. Examples of current interest include colloids [11] or cold atoms [12] in optical traps, superconducting vortices in lithographed tracks [13], ion-channels [14], cell membranes [15], artificial and natural nanopores [16], etc.

This paper is organized as follows: In Sec. II we introduce the model, define the units and give the details of our numerical simulations. Our numerical results are presented in Sec. III. In particular, the role of the dimer length in the transport properties is studied in Sec. III A; the monomer like regimes (for weak and strong couplings) are discussed in Sec. III B; finally, the influence of the coupling strength and of the damping constant on the dimer transport are analyzed in Sec. III C. Potential applications of our results to 1D irreducible devices are sketched in Sec. IV.

II. MODEL

A monomer moving on a 1D periodic substrate with potential $U_0(x) = U_0(x + L)$ under the influence of an external dc bias F and at finite temperature T can be described by the Langevin equation (LE),

$$m\ddot{x} = -\eta\dot{x} - \frac{dU_0(x)}{dx} + F + \xi(t). \quad (1)$$

Here $\eta = m\gamma$ is the viscous friction coefficient, with γ being a damping constant and m the mass of the Brownian particle. The stochastic force $\xi(t)$ represents the environmental fluctuations and is modeled by a Gaussian white noise with zero mean, $\langle \xi(t) \rangle = 0$, and auto-correlation function (ACF),

$$\langle \xi(t) \xi(t') \rangle = 2\eta k_B T \delta(t - t'). \quad (2)$$

For a symmetric dimer the corresponding LE's have the form

$$\begin{aligned} m\ddot{x}_1 &= -\eta\dot{x}_1 - \frac{\partial U(x_1, x_2)}{\partial x_1} + F + \xi_1(t), \\ m\ddot{x}_2 &= -\eta\dot{x}_2 - \frac{\partial U(x_1, x_2)}{\partial x_2} + F + \xi_2(t), \end{aligned} \quad (3)$$

where $\xi_i(t)$, $i = 1, 2$, are two independent zero-mean stochastic processes with ACF,

$$\langle \xi_i(t) \xi_j(t') \rangle = 2\eta k_B T \delta_{ij} \delta(t - t'). \quad (4)$$

Note that the inter-particle interaction is incorporated in the potential function,

$$U(x_1, x_2) = U_0(x_1) + U_0(x_2) + \frac{K}{2}(x_2 - x_1 - a_0)^2. \quad (5)$$

That is, we assume the interaction between the two dimer particles to be harmonic with coupling constant K and equilibrium distance a_0 . The simplest choice for the periodic substrate potential is [17],

$$U_0(x) = A_0 \cos(kx), \quad (6)$$

with $k = 2\pi/L$.

The LE's (1) and (3) can be conveniently rescaled. By introducing suitable space, energy, and time units,

$$\lambda = 1/k, \quad \epsilon = A_0, \quad \tau = \sqrt{\lambda^2 m / \epsilon}, \quad (7)$$

we define the dimensionless quantities:

$$\begin{aligned} \tilde{x} &= \frac{x}{\lambda}, & \tilde{a}_0 &= \frac{a_0}{\lambda}, & \tilde{T} &= \frac{k_B T}{\epsilon}, & \tilde{F} &= \frac{\lambda}{\epsilon} F, \\ \tilde{K} &= \frac{\lambda^2}{\epsilon} K, & \tilde{t} &= \frac{t}{\tau}, & \tilde{\gamma} &= \gamma \tau, & \tilde{\xi}(\tilde{t}) &= \frac{\lambda}{\epsilon} \xi(t). \end{aligned} \quad (8)$$

No particle can be trapped by the potential (6) under any circumstances for tilting larger than the critical value $\tilde{F}_{\text{cr}} = 1$ (in rescaled units). In the following we drop the tilde altogether.

After rescaling, the LE (1) for a monomer moving in the potential (6) reads,

$$\ddot{x} = -\gamma \dot{x} + \sin x + F + \xi(t), \quad (9)$$

where the ACF of the rescaled noise is $\langle \xi(t) \xi(t') \rangle = 2\gamma T \delta(t - t')$. Analogously, the coupled LE's (3) for a symmetric harmonic dimer in the same substrate potential become [see Eq. (5)],

$$\begin{aligned} \ddot{x}_1 &= -\gamma \dot{x}_1 + \sin x_1 + F + K(x_2 - x_1 - a_0) + \xi_1(t), \\ \ddot{x}_2 &= -\gamma \dot{x}_2 + \sin x_2 + F - K(x_2 - x_1 - a_0) + \xi_2(t), \end{aligned} \quad (10)$$

with $\langle \xi_i(t) \xi_j(t') \rangle = 2\gamma T \delta_{ij} \delta(t - t')$.

The dimensionless LE (9) for a monomer and (10) for a dimer have been integrated numerically through a standard Milstein algorithm [18]. Individual stochastic trajectories were simulated for different time lengths t_{max} and time steps Δt , so as to ensure appropriate numerical accuracy. Average quantities have been obtained as ensemble averages over 10^4 trajectories; transient effects have been estimated and subtracted.

III. RESULTS: MOBILITY AND DIFFUSION

When considering a pair of interacting Brownian particles, it is natural to study the motion of their center of mass,

$$X = \frac{1}{2}(x_1 + x_2). \quad (11)$$

The quantities that best characterize the stationary dimer flow are: (a) the net velocity,

$$v = \lim_{t \rightarrow \infty} \frac{\langle X(t) \rangle}{t}, \quad (12)$$

or, equivalently, the related mobility, $\mu = v/F$; (b) the diffusion coefficient,

$$D = \lim_{t \rightarrow \infty} \frac{\langle \delta X^2(t) \rangle}{2t}, \quad (13)$$

where $\langle \delta X^2 \rangle$ is the mean square displacement of the center of mass, i.e.,

$$\begin{aligned} \langle \delta X^2 \rangle &= \langle X^2 \rangle - \langle X \rangle^2 \\ &= \frac{1}{4} \langle \delta x_1^2 \rangle + \frac{1}{4} \langle \delta x_2^2 \rangle + \frac{1}{2} (\langle x_1 x_2 \rangle - \langle x_1 \rangle \langle x_2 \rangle). \end{aligned} \quad (14)$$

For the following discussion we also introduce the relative coordinate Y ,

$$Y = x_2 - x_1, \quad (15)$$

representing the dimer size. The quantity Y can in principle also become also negative. However, this happens only when the dimer oscillations around the equilibrium position become very large. In the range of parameters adopted in the present paper, we have verified that Y remains positive even for small values of the elastic constant K , where one recovers the monomer limit. In fact, the distance Y can become negative if both monomers fall into the same valley. In our simulations, the dimer length (at rest) varies in the range $a_0 \in [L, 2L]$. Thus, the monomers start out in different potential valleys and are observed to stay so for all times (i.e., configurations with $Y < 0$ do not occur).

The LE's (3) can be rewritten as a LE for the center of mass coordinate X and one for the dimer length Y , that is,

$$\begin{aligned} \ddot{X} &= -\gamma \dot{X} + \cos(Y/2) \sin X + F + Q(t)/\sqrt{2}, \\ \ddot{Y} &= -\gamma \dot{Y} + 2 \cos X \sin(Y/2) - 2K(Y - a_0) + \sqrt{2}q(t). \end{aligned} \quad (16)$$

Note that the two noises $Q(t) = [\xi_1(t) + \xi_2(t)]/\sqrt{2}$ and $q(t) = [\xi_2(t) - \xi_1(t)]/\sqrt{2}$ are uncorrelated and have the same statistics as $\xi_{1,2}(t)$, namely, $\langle q(t) \rangle = \langle Q(t) \rangle = 0$ and

$$\langle q(t)q(t') \rangle = \langle Q(t)Q(t') \rangle = 2\gamma T \delta(t - t'). \quad (18)$$

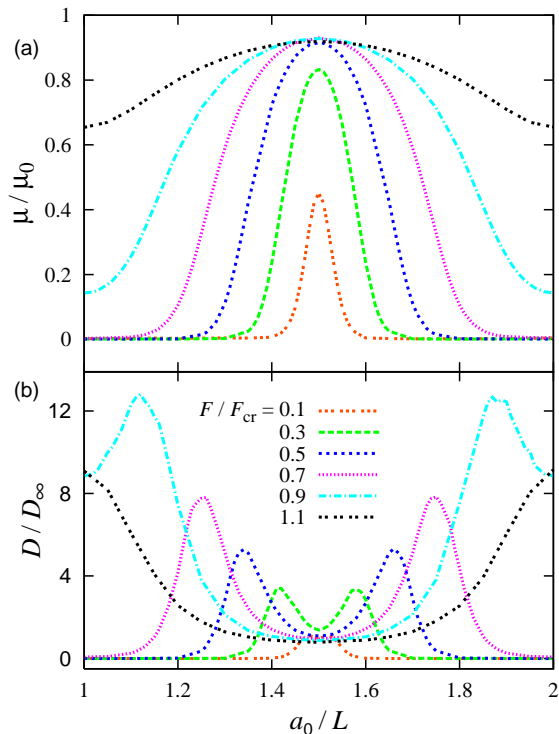


Figure 1: (Color online) Mobility (a) and diffusion coefficient (b) versus the dimer length a_0 for different values of the tilting force F . Simulation parameters: coupling constant $K = 1.5$, temperature $T = 0.1$ and $\gamma = 1$. D_∞ is the free dimer diffusion coefficient $D_\infty = D_0(T/2)$; see text.

In the absence of a substrate potential the mobility of both a monomer and a dimer is $\mu_0 = 1/\gamma$. Correspondingly, the free diffusion coefficient for a monomer, $D_0(T) \equiv T/\gamma$, is twice as large as that for a dimer, $D_0(T/2)$.

A. The role of the dimer length

At variance with a monomer, a dimer has two degrees of freedom. This affects its diffusion dynamics [19] to the point that its diffusion coefficient D can develop a non-monotonic dependence on the dimer parameters. For instance, dimer transport strongly depends on the ratio between the period L of the substrate and the natural length a_0 of the dimer [20, 21, 22].

In the absence of an external force, $F = 0$, at low temperature the diffusion coefficient of a rigid dimer decreases monotonically on raising the dimer length a_0 from $L/2$ to L . This can be well understood from Eq. (16). In the limit $K = \infty$ the dimer length is just $Y = a_0$ and the force $\cos(Y/2) \sin X$ acting on $X(t)$, Eq. (16), corresponds to a periodic potential with amplitude $|\cos(Y/2)|$. For $a_0 = L/2 = \pi$ this quantity is zero and the dimer center of mass undergoes free diffusion.

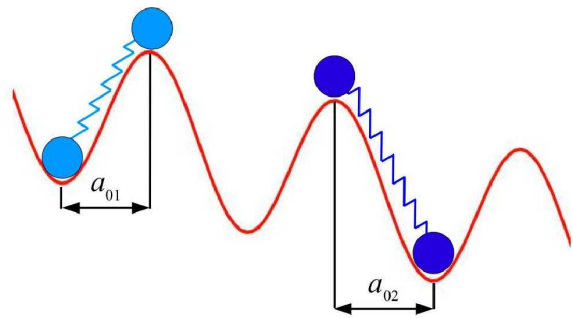


Figure 2: (Color online) Dimer configurations corresponding to zero pinning force and maximum diffusion coefficient; see also Fig. 1 and text.

For $a_0 = L = 2\pi$ the periodic potential amplitude is maximum, $|\cos(Y/2)| = 1$; diffusion in a periodic potential is known to be suppressed compared to free diffusion [23, 24]. Therefore, the maxima and minima of D versus a_0 coincide with the minima and the maxima of the modulating factor $|\cos(a_0/2)|$, respectively. This conclusion applies also to the case of finite elastic constants as long as $\langle Y(t) \rangle \approx a_0$, that is for rigid dimers, $K \gg 1$, at low temperatures, $T \ll 1$. (For the opposite limit of weak dimers, $K \ll 1$, see Sec. III B.)

In the presence of a sub-threshold external force, $F < F_{\text{cr}}$, the diffusion coefficient D is a nonmonotonic function of the dimer length a_0 , as shown in Fig. 1(b). The numerical results in Fig. 1 have been obtained by simulating a relatively rigid, $K = 1.5$, and moderately damped, $\gamma = 1$, dimer. In the case of a strongly to moderately damped *monomer* in a washboard potential, the curves $D(F, T)$ are known to develop a peak around F_{cr} , where the barrier height of the tilted periodic potential $U_0(x) - Fx$ vanishes [25]. Analogously, in the case of a dimer, D attains a maximum for dimer lengths such that the effective pinning force also vanishes, i.e., for a_0 equal to the distances between maxima and minima of the washboard potential, see Fig. 2. In the case of a driven rigid dimer with $F < F_{\text{cr}} = 1$, this takes place for equilibrium lengths $a_0^\pm = (L/2)[1 \pm (2/\pi) \arcsin(F)]$. Note that a_0^\pm are given mod(L) and $a_0^+ + a_0^- = L$.

Figure 1(a) demonstrates that the mobility is smallest for commensurate dimers with $a_0 = L$ and largest for $a_0 = L/2$ (see also Ref. [22]). The smaller the applied constant force, the smaller is the a_0 range around $a_0 = L/2$, where the mobility of the dimer is significantly different from zero. For large enough tilting the dimer is considerably mobile, no matter what is the value of a_0 . For $F \rightarrow \infty$ the mobility $\mu \rightarrow \mu_0$ and the effective diffusion coefficient $D \rightarrow D_\infty = D_0(T/2)$. We remark that the a_0 dependencies of μ and D shown in Fig. 1 are given mod(L) [22]. In fact, the system dynamics, as given by Eqs. (10), is invariant under the change $a_0 \rightarrow a_0 + L$ and $x_1 \rightarrow x_1 - L$ (or $x_2 \rightarrow x_2 + L$).

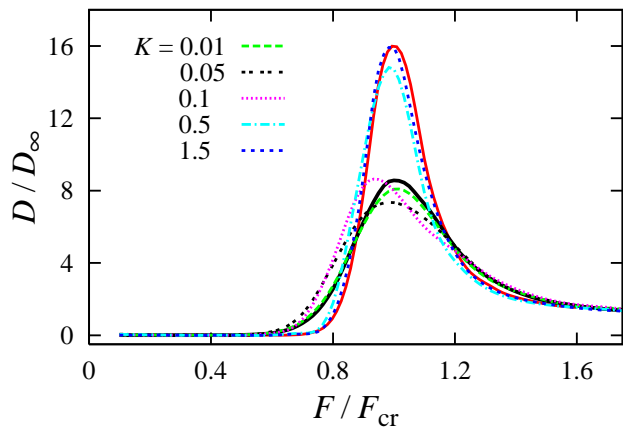


Figure 3: (Color online) Diffusion coefficient D versus the tilting force F for a dimer length $a_0/L = 1$ and different coupling constants K ; $T = 0.1$ and $\gamma = 1$. The corresponding curves for monomers of temperature T (solid, black) and $T/2$ (solid, red) are drawn for comparison (see text).

B. Monomer like regimes

In the case of a monomer the mobility and the diffusion in a tilted periodic potential are in general well understood. In the low-temperature regime, $T \ll 1$, the particle mobility is close to zero for sub-threshold tilting (locked state). Around a depinning threshold F_d , the mobility grows sharply and in the large force limit reaches the free particle limit μ_0 (running state). If the temperature is increased, the transition from the locked to the running state is smoother. In the overdamped regime, convenient fully analytical expressions are available for both the mobility $\mu(F, T)$ (the Stratonovich formula [26]) and the diffusion coefficient $D(F, T)$ (the Cox formula [27]). For small biases and low temperature, the diffusion coefficient is suppressed compared to the free diffusion $D_0(T)$; in linear response theory $D(F, T) \simeq \mu(F, T)T$ [17]. Depinning occurs around the critical tilt, i.e., $F_d \simeq F_{cr}$, as signaled by $D(F, T)$ overshooting D_0 [25]; the lower the temperature, the more prominent is the growth of the depinning diffusion peak. In the large force limit, the free diffusion regime $D_0(T)$ is eventually recovered.

In the underdamped limit, $\gamma \ll \sqrt{F_{cr}}$, the mobility and the diffusion coefficient display a similar behavior with one significant difference: the depinning threshold F_d is a monotonic function of the damping constant with

$$\lim_{\gamma \rightarrow 0} F_d \simeq 3.36\gamma\sqrt{F_{cr}} \quad (19)$$

and $F_d \simeq F_{cr}$ for $\gamma \gtrsim \sqrt{F_{cr}}$ [17, 28].

In the case of a dimer, the general behavior recalls that of a monomer, namely, both the transition of the rescaled mobility from 0 to μ_0 and the corresponding enhance-

ment of the diffusion coefficient above its free diffusion value still occur as the tilting force is increased past the depinning threshold. The monomer dynamics is a useful benchmark to check the accuracy of our simulations for the dimer diffusion. Indeed, in the limit $K \rightarrow 0$, Eq. (15) boils down to $\langle \delta X^2 \rangle = \langle \delta x_1^2 \rangle / 2$, with x_1 obeying the monomer LE (9) with temperature T . It follows that for a weak dimer, $K \ll 1$, the ratio D/D_∞ is closely reproduced by the analytical curve $D(F, T)/D_0(T)$ obtained from the monomer LE (9). This argument applies to both commensurate, Fig. 3, and incommensurate dimers, Fig. 4(b).

Rigid dimers also behave like monomers. In the limit $K \rightarrow \infty$, the solution of Eq. (17) is $Y(t) \equiv Y = a_0$ and Eq. (16) is then equivalent to the monomer LE (9) with temperature $T/2$ and substrate amplitude (critical tilt) $\cos(a_0/2)$. Accordingly, for commensurate dimers with a_0 equal to an integer multiple of the substrate constant L , the ratio D/D_∞ is reproduced by the curve $D(F, T/2)/D_0(T/2)$ obtained for a monomer on a tilted cosine potential with amplitude $|\cos(a_0/2)| = 1$ and temperature $T/2$ (see Fig. 3).

Note that for large values of damping the monomer curve can also be computed analytically through the Cox formula [27]. The data in Fig. 3 confirm that for increasingly large K the depinning threshold approaches $F_{cr} = 1$ from below, as the effective critical tilt $\langle |\cos(\psi/2)| \rangle$ tends to unity. Not surprisingly, for the commensurate dimer of Fig. 3 the mobility curve coincides with the monomer mobility $\mu(F, T)$, in the weak coupling limit, and with the monomer mobility at half the temperature T , $\mu(F, T/2)$, in the strong coupling limit; both limiting curves are closely approximated by the Stratonovich formula (not shown).

For $K \rightarrow \infty$ incommensurate dimers behave like monomers moving on a tilted cosine potential with amplitude $|\cos(a_0/2)| < 1$ and temperature $T/2$ (see also Fig. 5 for a finite coupling). When a_0 is equal to a half-integer multiple of the substrate constant L , the amplitude of the effective substrate acting on the dimer coordinate X vanishes, $|\cos(a_0/2)| = 0$, and the dimer diffusion becomes insensitive to the substrate, with mobility μ_0 and diffusion coefficient $D_0(T/2)$.

Figures 4 and 5 indicate that for a finite K the dimers exhibit a much more complicated behavior, which will be discussed in the forthcoming section.

C. The dependence on the coupling strength

The problem of a dimer diffusing in a washboard potential has been studied in fact in many papers, but due to the large parameter space, important effects went unnoticed. In Ref. [29], it was found that for a commensurate dimer, $D(F, T)$ had two maxima as a function of the tilting force F , whereas an incommensurate dimer behaved more like a monomer, with D showing only one peak. However, as shown in Fig. 4(b), one can observe two F

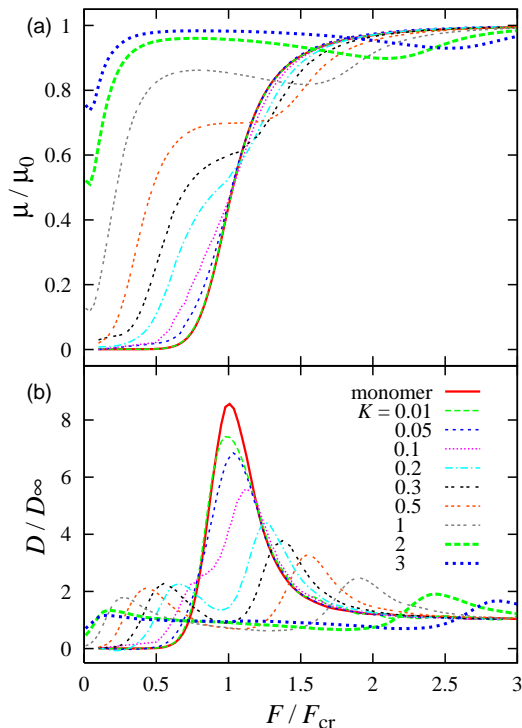


Figure 4: (Color online) Mobility (a) and diffusion coefficient (b) versus the tilting force F for an equilibrium distance $a_0/L = 1.5$ and for different values of the coupling constant K ; $T = 0.1$ and $\gamma = 1$. In both panels the results are compared with the corresponding monomer curves (see text).

maxima also in the diffusion coefficient of a noncommensurate dimer; correspondingly, the mobility curve μ versus F develops the nonmonotonic behavior displayed in Fig. 4(a). More remarkably, for the same temperature and damping constant of Fig. 4, commensurate dimers presented a single peaked diffusion coefficient and monotonic mobility as functions of the tilt (see Figs. 3 and 5). However, for different simulation parameters (like those in Ref. [29]) two-peaked D curves were detected for commensurate dimers, as well. Thus, a doubly peaked diffusion coefficient is no signature of dimer-substrate commensuration: the coupling constant (Fig. 4), damping constant (Fig. 6), and temperature also play a significant role [see Eqs. 22 and 23].

To investigate the origin of the two competing diffusion mechanisms shown in Fig. 4, we address in detail the case of a dimer with length a_0 equal to a half-integer multiple of the substrate constant L . For a finite coupling strength K , on setting $Y(t) = a_0 + \psi(t)$, the coupled LE's (16) and (17) read

$$\ddot{X} = -\gamma\dot{X} - \sin(\psi/2)\sin X + F + Q(t)/\sqrt{2}, \quad (20)$$

$$\ddot{\psi} = -\gamma\dot{\psi} + 2\cos(\psi/2)\cos X - 2K\psi + \sqrt{2}q(t). \quad (21)$$

If the dimer is sufficiently rigid and the tilting force F

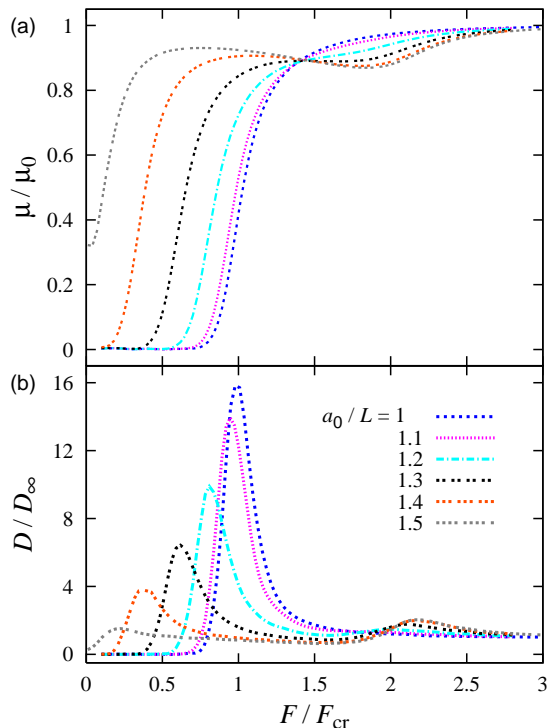


Figure 5: (Color online) Mobility (a) and diffusion coefficient (b) versus the tilting force F for a coupling constant $K = 1.5$ and for different values of the equilibrium distance a_0 . T and γ have the same values as in Figs. 4 and 3.

weak, then $\psi(t)$ is small and mostly controlled by thermal noise. From Eq. (21), on neglecting the substrate force with respect to the dimer coupling, energy equipartition yields $\langle\psi^2(t)\rangle = T/K$. Moreover, the force term $\sin(\psi/2)\sin X$ in Eq. (20) can be treated as resulting from a randomly flashing cosine potential with amplitude $2|\langle\sin[\psi(t)/2]\rangle| \approx |\psi|$. This can be regarded as an instance of the “parametric resonance” approach pursued by the authors of Ref. [20] in the limit $T = 0$. On assuming a Gaussian distribution for ψ , a corresponding γ -independent effective critical tilt can thus be estimated, namely,

$$F_1 \approx [(2/\pi)\langle\psi^2(t)\rangle]^{1/2} = \sqrt{2T/\pi K}. \quad (22)$$

As pointed out in Sec. III B, for large to intermediate values of damping, the critical tilt coincides with the effective dimer depinning threshold F_d . For $K \geq 0.2$, Eq. (22) locates rather accurately the first F peak of the simulated diffusion coefficient reported in Fig. 4(b).

For $F > F_1$ both the dimer mobility and the diffusion coefficient tend towards their free particle values, unless an internal resonance sets in. Indeed, driven by a strong force F , the dimer center of mass acquires an almost constant speed F/γ . On inserting $X(t) \simeq Ft/\gamma$ into its right hand side, Eq. (21) becomes the LE of a

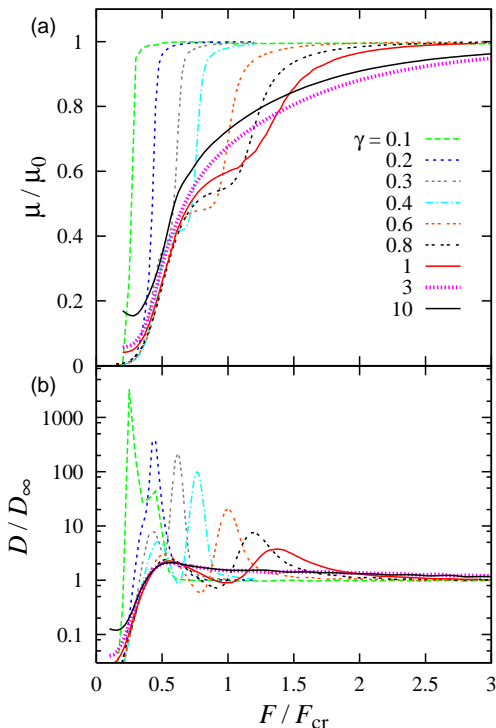


Figure 6: (Color online) Mobility (a) and diffusion coefficient (b) versus the tilting force F for $a_0/L = 1.5$ and different values of damping constant γ ; $T = 0.1$ and $K = 0.3$. Two-peaked diffusion curves are clearly distinguishable for $\gamma \leq 1$ only.

Brownian oscillator subjected to a harmonic force with angular frequency $\Omega = F/\gamma$. Accordingly, the internal degree of freedom of the dimer, represented by the coordinate Y , resonates for F/γ approaching $\sqrt{2K - \gamma^2/2}$ (parametric resonance [20, 29, 30, 31]), thus leading to a threshold-like enhancement of the dimer diffusion [25]. Our argument can be refined further by noticing that at resonance the processes $X(t)$ and $\psi(t)$ synchronize their phases, so that the substrate force in Eq. (20) does not average out any more. In the presence of synchronization, $\langle \sin(\psi/2) \sin X \rangle \simeq 1/2$, which amounts to replacing F with $F - 1/2$. In conclusion, for relatively large damping constants, namely $1 \lesssim \gamma < 2\sqrt{K}$, a resonance diffusion F peak is expected for

$$F_2 \approx \frac{1}{2} + \gamma \sqrt{2K - \frac{\gamma^2}{2}}. \quad (23)$$

in reasonable agreement with the simulation results of Fig. 4(b) for $\gamma = 1$. Correspondingly, the mobility curves describe a two step transition from the locked to the running state.

For weak dimers, $K < (\gamma/2)^2$, the two peaks of the diffusion coefficient tend to merge, as shown in Fig. 4(b), and in the limit $K \rightarrow 0$ a monomer dynamics is recovered

(see Sec. III B). Equivalently, incommensurate dimers with $\gamma > 2\sqrt{K}$ must be regarded as overdamped as far as their internal coordinate Y is concerned; therefore, their diffusion coefficients are characterized by one maximum located around the γ -independent depinning threshold F_d in Eq. (22); see Fig. 6(b). When γ decreases, both diffusion peaks shift towards smaller values of F . The explanation is very simple: The resonance threshold F_2 tends almost linearly to $1/2$; in the underdamped regime, the depinning threshold F_d is proportional to γ as it obeys law (19) with F_{cr} given by the effective critical tilt F_1 of Eq. (22). This estimate for F_d in the underdamped limit is consistent with the anticipated locked-to-running transition thresholds exhibited by the mobility curves of Fig. 6(a) with $\gamma \lesssim 0.3$.

Going back to the dynamics of the damped incommensurate dimer of Fig. 4, we remark that on increasing K the resonance diffusion peaks, in addition to shifting to higher F (directly proportional to \sqrt{K}), flatten out on top of the plateau $D = D_0(T/2)$; as the depinning peaks move to lower F (inversely proportional to \sqrt{K}), for $K \rightarrow \infty$ the diffusion coefficient eventually tends to $D_0(T/2)$, as anticipated in the previous Sections.

The argument presented here can be easily generalized to the case of commensurate dimers, or to any equilibrium length; the ensuing properties of commensurate versus noncommensurate dimers and the different monomer limits of the dimer dynamics have been anticipated, respectively, in Secs. III A and III B.

IV. CONCLUSION

In this paper we have studied a system consisting of two harmonically interacting Brownian particles diffusing in a 1D washboard potential. We found that the average current and the diffusion coefficient of such a dimer exhibit a complicated non-monotonic behavior as a function of the driving force and the ratio of the dimer length to substrate constant. In the limits of the weak ($K \rightarrow 0$) and strong ($K \rightarrow \infty$) coupling constant the expected monomer dynamics was recovered. Moreover, we studied in detail the dimer transport for different coupling strengths and damping constants. We concluded that the appearance of the second resonant peak of the diffusion coefficient versus the driving force is not related to the dimer length-to-substrate constant ratio, but rather to the damping-to-coupling constant ratio; the diffusion coefficient $D(F)$ possesses two peaks only for relatively low damping values.

Finally, we recall that a simple 1D model is not always a viable tool to analyze transport in two or higher dimensions: such a modeling makes sense for highly symmetric substrates, only. There exist irreducible 2D and 3D devices where particles are driven on an *asymmetric* potential landscape by an ac or dc driving force perpendicularly to the symmetry axis of the potential. Such a geometry has recently attracted broad interest [32] in the

context of separation of macromolecules, DNA, or even cells, because it is capable of inducing a transverse drift as a function of the drive and of the particle geometry: as a consequence different objects can be separated depending on their center of mass diffusion coefficient [33]. While the motivations of the present study apply to this class of devices, too, it is clear that their characterization must take into account the dimensionality of the system at hand. Dimensional reduction is limited by the spatial symmetry of the substrate and the particles. This is the

subject of ongoing investigation.

Acknowledgments

This work has been supported by the Estonian Science Foundation via Grant No. 6789 and by the Archimedes Foundation (EH).

-
- [1] J.W.M. Frenken and J.F. van der Veen, *Phys. Rev. Lett.* **54**, 134 (1985); B. Pluis, A.W. Denier van der Gon, J.W.M. Frenken, J.F. van der Veen, *ibid.* **59**, 2678 (1987); D.C. Senft and G. Ehrlich, *ibid.* **74**, 294 (1995); T.R. Linderoth, S. Horch, E. Laegsgaard, I. Stensgaard, and F. Besenbacher, *ibid.* **78**, 4978 (1997); P. Talkner, E. Hershkovitz, E. Pollak, and P. Hänggi, *Surf. Sci.* **437**, 198 (1999); M. Borromeo and F. Marchesoni, *ibid.* **465**, 235 (2000).
- [2] A.G. Naumovets and Yu.S. Vedula, *Surf. Sci. Rep.* **4**, 365 (1985); R. Gomer, *Rep. Prog. Phys.* **53**, 917 (1990).
- [3] M. Porto, M. Urbakh, and J. Klafter, *Phys. Rev. Lett.* **84**, 6058 (2000).
- [4] S.C. Wang and G. Ehrlich, *Surf. Sci.* **239**, 301 (1990); G.L. Kellogg, *Appl. Surf. Sci.* **67**, 134 (1993); S.C. Wang and G. Ehrlich, *Phys. Rev. Lett.* **79**, 4234 (1997); S.C. Wang, U. Kürpick, and G. Ehrlich, *ibid.* **81**, 4923 (1998).
- [5] A.F. Voter, *Phys. Rev. B* **34**, 6819 (1986); C.-L. Liu and J.B. Adams, *Surf. Sci.* **268**, 73 (1992); C. Massobrio and P. Blandin, *Phys. Rev. B* **47**, 13687 (1993); J.C. Hamilton, M.S. Daw, and S.M. Foiles, *Phys. Rev. Lett.* **74**, 2760 (1995); Clinton DeW. Van Siclen, *ibid.* **75**, 1574 (1995); S.V. Khare, N.C. Bartelt, and T.L. Einstein, *ibid.* **75**, 2148 (1995); D.S. Sholl and R.T. Skodje, *ibid.* **75**, 3158 (1995).
- [6] A.G. Naumovets and Z. Zhang, *Surf. Sci.* **500**, 414 (2002).
- [7] T. Ala-Nissila, R. Ferrando, and S.C. Ying, *Adv. Phys.* **51**, 949 (2002).
- [8] B.S. Swartzentruber, *Phys. Rev. Lett.* **76**, 459 (1996); W. Wulfhekel, B.J. Hattink, H.J.W. Zandvliet, G. Rosenfeld, and B. Poelsema, *ibid.* **79**, 2494 (1997); H.J.W. Zandvliet, T.M. Galea, E. Zoethout, and B. Poelsema, *ibid.* **84**, 1523 (2000).
- [9] S. Savel'ev, F. Marchesoni, and F. Nori, *Phys. Rev. Lett.* **91**, 010601 (2003); *ibid.* **92**, 160602 (2004).
- [10] A. H. Romero, A. M. Lacasta, and J. M. Sancho, *Phys. Rev. E* **69**, 051105 (2004).
- [11] Q.H. Wei, C. Bechinger, and P. Leiderer, *Science* **287**, 625 (2000); C. Lutz, M. Kollmann, and C. Bechinger, *Phys. Rev. Lett.* **93**, 026001 (2004).
- [12] R. Gommers, S. Denisov, and F. Renzoni, *Phys. Rev. Lett.* **96**, 240604 (2006); R. Gommers, S. Bergamini, and F. Renzoni, *ibid.* **95**, 073003 (2005).
- [13] A. Tonomura, *Rev. Mod. Phys.* **59**, 639 (1987); J.F. Wambaugh, C. Reichhardt, C.J. Olson, F. Marchesoni, and F. Nori, *Phys. Rev. Lett.* **83**, 5106 (1999).
- [14] D.A. Doyle, J.M. Cabral, R.A. Pfuetzner, A. Kuo, J.M. Gulbis, S.L. Cohen, B.T. Chait, and R. MacKinnon, *Science* **280**, 69 (1998).
- [15] B. Alberts *et al.*, *Molecular Biology of the Cell* (Garland, New York, 1994).
- [16] J. Kärger and D.M. Ruthven, *Diffusion in Zeolites and Other Microporous Solids* (Wiley, New York, 1992); S. Matthias and F. Müller, *Nature* **424**, 53 (2003); Z. Siwy and A. Fulinski, *Phys. Rev. Lett.* **89**, 198103 (2002); C. Kettner, P. Reimann, P. Hänggi, F. Müller, *Phys. Rev. E* **61**, 312 (2000).
- [17] H. Risken, *The Fokker-Planck Equation* (Springer, Berlin, 1984). Chap. 11.
- [18] P.E. Kloeden and E. Platen, *Numerical Solution of Stochastic Differential Equations* (Springer, Berlin, 1999).
- [19] O.M. Braun, *Phys. Rev. E* **63**, 011102 (2000).
- [20] C. Fusco and A. Fasolino, *Thin Solid Films* **428**, 34 (2003).
- [21] O.M. Braun, *Surf. Sci.* **230**, 262 (1990).
- [22] M. Patriarca, P. Szelestey, and E. Heinsalu, *Acta Phys. Pol. B* **36**, 1745 (2005).
- [23] S. Lifson, J.L. Jackson, *J. Chem. Phys.* **36**, 2410 (1962).
- [24] R. Festa, E.G. d'Agliano, *Physica A* **90**, 229 (1978).
- [25] G. Costantini and F. Marchesoni, *Europhys. Lett.* **48**, 491 (1999).
- [26] R.L. Stratonovich, *Radiotekh. Electron. (Moscow)* **3**, 497 (1958). English translation in *Non-Linear Transformations of Stochastic Processes*, edited by P.I. Kuznetsov, R.L. Stratonovich, and V.I. Tikhonov (Pergamon, Oxford, 1965).
- [27] D.R. Cox, *Renewal Theory* (Methuen & Co., London, 1962), Chap. 5; P. Reimann, C. Van den Broeck, H. Linke, P. Hänggi, J.M. Rubi, and A. Pérez-Madrid, *Phys. Rev. Lett.* **87**, 010602 (2001); B. Lindner, M. Kostur, and L. Schimansky-Geier, *Fluct. Noise Lett.* **1**, R25 (2001).
- [28] M. Borromeo, G. Costantini, and F. Marchesoni, *Phys. Rev. Lett.* **82**, 2820 (1999).
- [29] O.M. Braun, R. Ferrando, and G.E. Tommei, *Phys. Rev. E* **68**, 051101 (2003).
- [30] T. Strunz, F.-J. Elmer, *Phys. Rev. E* **58**, 1601 (1998).
- [31] C. Cattuto and F. Marchesoni, *Phys. Rev. Lett.* **79**, 5070 (1997).
- [32] D. Ertas, *Phys. Rev. Lett.* **80**, 1548 (1998); A. Oudenaarden and S.G. Boxer, *Science* **285**, 1046 (1999). L.R. Huang, P. Silberzan, J.O. Tegenfeldt, E.C. Cox, J.C. Sturm, R.H. Austin, and H. Craighead, *Phys. Rev. Lett.* *Phys. Rev. Lett.* **89**, 178301 (2002); M. Berger, J. Castelino, R. Huang, M. Shah, and R.H. Austin, *Electrophoresis* **22**, 3883 (2001).

- [33] S. Savel'ev, V. Misko, F. Marchesoni, and F. Nori, Phys. Rev. B **71**, 214303 (2005).